metals

MDPI

Article

An Inherent Strain Method Using Progressive Element Activation for Fast Distortion Calculation in Directed Energy Deposition

Georg Seitz [1,*], Patrick Bantle [1], Max Biegler [1], Beatrix A. M. Elsner [2] and Michael Rethmeier [1,3,4]

[1] Fraunhofer Institute for Production Systems and Design Technology (IPK), 10587 Berlin, Germany
[2] Hexagon Manufacturing Intelligence GmbH, 21079 Hamburg, Germany
[3] Bundesanstalt für Materialforschung und -prüfung (BAM), 12205 Berlin, Germany
[4] Institute for Machine Tools and Factory Management (IWF), Technical University of Berlin, 10587 Berlin, Germany
* Correspondence: georg.seitz@ipk.fraunhofer.de; Tel.: +49-30-39006-218

Abstract: The finite element analysis (FEA) simulation of directed energy deposition (DED) processes offers many potential cost savings during the build job optimization process, through, e.g., distortion predictions. However, the biggest challenge is the long calculation time, frequently exceeding the actual build time. One way of simplifying the simulation with the aim of reducing the calculation times is the inherent strain method. While this method is already used commercially in the simulation of powder bed-based processes and conventional welding technologies, its use in DED is still the subject of research. In this work, an inverse determination of an inherent strain is carried out on a 20-layer-high, single-track-wide wall, common theories are reviewed, and an approach based on thermal strain is introduced. As a result, the calculation time could be reduced by 83% and the accuracy remained at 92%.

Keywords: inherent strain method; simulation; finite element analysis; directed energy deposition; additive manufacturing

Citation: Seitz, G.; Bantle, P.; Biegler, M.; Elsner, B.A.M.; Rethmeier, M. An Inherent Strain Method Using Progressive Element Activation for Fast Distortion Calculation in Directed Energy Deposition. *Metals* **2024**, *14*, 1338. https://doi.org/10.3390/met14121338

Academic Editor: Daniela Pilone

Received: 8 October 2024
Revised: 11 November 2024
Accepted: 18 November 2024
Published: 26 November 2024

1. Introduction

Additive manufacturing (AM) is increasingly finding its way into industrial practice, as it offers the construction of complex geometries with near-net-shape moulding and great design freedom compared to established machining approaches. Directed energy deposition (DED) is an AM processes that enables complex components to be created by welding several layers of material on top of each other, whereby welded material can be supplied in the form of powder or wire [1]. The process can further be categorized by the used heat sources: wire arc additive manufacturing (WAAM) provides a higher deposition rate, whereas laser beam DED (also known as LENS: Laser Engineered Net Shaping) provides the highest detail resolution [2]. During the build-up process, the substrate as well as the already applied layers are heated cyclically due to the addition of further welds. This results in complex states of multiple stages of heating, cooling, expansion, shrinkage, and, finally, distortion and residual stresses. If complex components such as gas turbine components are built, the entire process is established experimentally and iteratively [3]. Time-consuming and costly trial and error is necessary to establish suitable process parameters, cooling times, and build paths. Also, often methodologies like Design of Experiments (DoE) are employed to determine useful parameter combinations experimentally [4]. Furthermore, it is even possible to compensate for distortions [5]; however, this requires further tests before an acceptable component quality can be guaranteed and the component can go into production. Numerical finite element analysis (FEA) simulations have the potential to reduce this experimental effort by performing virtual optimizations before experiments are carried out.

Biegler et al. [6], for example, carried out the geometric compensation of a turbine blade using only simulations. However, a limiting factor here is the long computation times, which often exceed the actual experimental build times. In his study, Biegler required a computing time of 36.6 h for the simulation, while the associated experimental build only required 1.2 h.

Various simplification methods exist in the FEA simulation of welding processes to overcome this problem. For example, Marimuthu et al. [7] utilized the rotational symmetry of a DED geometry to simplify the heat input. A layer-heating approach was used here, where equivalent amounts of energy are introduced simultaneously into the entire layer. By neglecting the transient movement of the heat source, the calculation time was reduced by 70%, whereas the quality of the results was not discussed and therefore the industrial application of the method is questionable. In a different approach, Biegler et al. [8] lowered the computational time by reducing the amount of contact bodies without sacrificing the accuracy of the transient approach. Another method of simplification used in the simulation of conventional welding is the inherent strain method (IS method), introduced by Yuan et al. [9]. They proposed the inherent strain to be the sum of the incompatible strains resulting from a welding process (e.g., plastic strain, shrinkage strain, creep strain, and phase transformation strain). They determined the inherent strain, based on various assumptions, only from the plastic strain from a thermomechanical calculation of a welding process and were able to use this to predict the residual stresses in a purely mechanical-elastic calculation. Liang et al. [10] argue that this methodology cannot be transferred to additive manufacturing processes, as the geometric boundary conditions are changed with the build-up of each new layer. As a result, Liang proposes the modified inherent strain, which includes the change in the elastic strain in addition to the plastic strain introduced at the time of material deposition. This change in elastic strain between two predefined time steps is supposed to represent the changing of the geometric boundary conditions. Liang [10] has applied this methodology to the DED structure of two-layer-high walls; however, they have only used the distortion of the substrate plate for validation. In his further research, Liang [11] also applied this approach to a DED structure of a five-layer wall where the modified IS method showed good result quality when comparing the inherent strain calculated distortion of the wall to the thermomechanical simulation. Duan et al. adopted Liang's approach and calculated the distortion of a substrate plate [12], a cam of a camshaft [13], and an entire camshaft in several investigations [14]. However, in the latter two investigations examining real components, the quality of the IS calculation was not evaluated by comparison with an experiment or a thermomechanical calculation. Bellet et al. [15], on the other hand, criticized Liang's approach, as Liang's determination of the inherent strain is not "direct, representative and systematic". Bellet therefore developed the extended approach of the inherent strain rate. Here, the inherent strain is recalibrated by a short section of thermomechanical calculation for each new layer. Afterwards, the layer is then finalized using the IS method.

Apart from the direct calculation of the inherent strain, there are also iterative inverse methods. Chen et al. [16] used the approach of an inverse determination of the inherent strain that is needed to calculate the known distortion of a DED component, and then compared the distortion of the substrate plate between the inherent strain calculation, thermomechanical calculation, and experiment. Ye et al. [17] also used an inverse identification of an inherent strain and validated the inherent strain calculation against an experiment, but distortions were also only measured on the substrate plate.

In the following, the application of an inherent strain method on DED simulation will be investigated with the goal of providing a suitable simplification method to reduce the calculation time while maintaining an acceptable result accuracy. Differently from the literature, an element-by-element application of the inherent strain is used. In the first step, it is examined whether the distortion of a wall can be calculated with a constant inherent strain using an inverse determination. Afterwards, the existing approaches for

the mathematical calculation of an inherent strain are examined and, due to a lack of applicability, a separate method based on thermal strain is developed.

2. Materials and Methods

2.1. Numerical Simulation

All finite element (FE) simulations were conducted in the commercial software Simufact Welding 2022.1 [18]. The simulation model is based on existing work that can be found in [19] and uses the same process parameters. The calibration used a metallographic cross section and transient temperature measurements in line with [20]. The material dataset for the utilized 316 L originates from the native material library of Simufact Welding [18]. This dataset is also described along with the chemical composition of the material and the governing equations of the simulation in previous works, which can be found in [19]. All investigations were carried out on a single weld track-wide wall depicted in Figure 1. The welding process is bidirectional, starting for the first layer in a positive x-direction and then alternating for every new layer. The whole baseplate was fixed during the weld cycles. The model consisted of 23,650 linear hexahedral elements. Each layer of the wall consists of two elements over the layer height and two elements over the width of the weld track. These boundary conditions resulted in an element edge length of 0.3 mm. The calculation duration for the thermomechanical solution took 9.5 h. A single refinement of the whole wall in the mesh convergence assessment resulted in an increased computational time of 17 h while only providing a 0.6% variation in the peak process temperature. A study of twofold refinement was not pursued due to the large computational times. Considering the marginal accuracy differences in regards to the peak temperature, the meshing of the base model was considered the most appropriate.

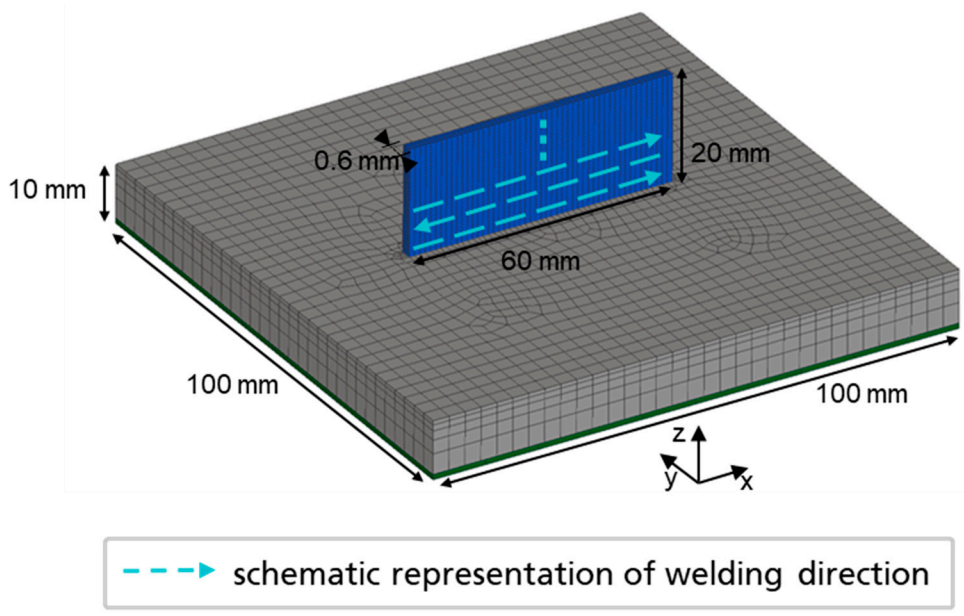

Figure 1. Geometric properties of the simulation model and path planning for the examined wall geometry. The first layer starts on the left-hand side of the wall and is finished on the right-hand side. Each following layer is then alternated.

2.2. Application of Inherent Strain Simulation

The inherent strain is applied in a transient manner element by element in this work. While in the literature, an entire layer is often activated at once and assigned an inherent strain, findings of Biegler [21] showed that using a layer-by-layer approach for thermomechanical simulations underestimates the bulging effects of distortion, especially around curves. For the application of the inherent strain in this work, analogous to thermomechanical implementations, a search volume follows the weld path and activates all elements

that are covered by the search volume. Instead of applying a heat input, the inherent strain vector is then applied to the activated elements. The geometric dimensions of the search volume correspond to the laser heat source in the thermomechanical simulation, which has a radius of 0.7 mm and a depth of 0.75 mm. Based on the search volume movement of 10 mm/s^{-1}, every increment activates 6 elements and applies the inherent strain to each of those elements. Upon the application of the inherent strain, the simulation calculates a nonlinear mechanical equilibrium in each increment, determining the material stress and part distortion. The inherent strain calculation is a purely mechanical calculation that uses a linear elastic material model, similarly to approaches found in the literature [9,10,13].

2.3. Form of the Inherent Strains

The choice of geometry is related to the selected investigation of the inherent strain. On a single-track-wide wall, the significant distortion occurs in the direction of longitudinal expansion, which corresponds to the weld path. Although there is transverse shrinkage, there is no distortion, as this would require the transverse shrinkage to be significantly geometrically impeded, which is not the case. The same applies to the distortion in the building direction (z-direction).

As a result, the inherent strain can be simplified to the following form:

$$\varepsilon^{Is} = \begin{pmatrix} x \\ y \\ z \end{pmatrix} \Rightarrow \varepsilon^{Is} = \begin{pmatrix} x \\ 0 \\ 0 \end{pmatrix}$$

The desired inherent strain can now be determined on this geometry initially by inverse determination in comparison to a thermomechanical calculation, and it can then be extended to a three-dimensional vector in subsequent works using more complex geometries, on which the interactions of the individual directional strains would be expected and distortions in several spatial directions are significant.

2.4. Inverse Calibration of the Inherent Strain

The inherent strain (IS) simulation is carried out with arbitrarily selected values for the inherent strain and is adapted according to the simulation results in a trial-and-error manner. The desired results for the distortion, which are the results from the thermomechanical simulation, are approximated iteratively. The target criteria are a qualitative and a quantitative comparison of the distortion. Qualitatively, the graphical distribution of the distortion of the thermomechanical simulation is to be achieved. The value of the maximum and minimum distortion in the x-direction of the thermomechanical simulation is used as a quantitative comparison criterion. The aim of the inverse calibration is to approach an arbitrary chosen deviation of less than 10% of the maximum and minimum distortion of the thermomechanical simulation.

2.5. Testing of Common Approaches

In this chapter, the formulas of the common approaches of the classic inherent strain (CIS) and the modified inherent strain (MIS) are used to determine the values for the inherent strain and to cross-check them with the previously inverse determined value. The entire first layer over the entire length of the wall is used as the location for the calculation of the inherent strain.

The following formulas are used to determine the two inherent strains. The classic inherent strain corresponds the approach of Yuan [9].

Classic inherent strain ε^{CIS}:

$$\varepsilon^{CIS} = \varepsilon^{Pl} = \varepsilon^{Pl}_{t_2}$$

where ε^{Pl} is the plastic strain at the end of the time taken to cool to room temperature. This corresponds to the plastic strain at the final state t_2 defined by Liang [10] for his approach of the modified inherent strain.

Modified inherent strain ε^{MIS}:

$$\varepsilon^{MIS} = \varepsilon^{Pl}_{t_1} + \varepsilon^{El}_{t_1} - \varepsilon^{El}_{t_2}$$

According to Liang [10], t_1 is selected to be the time point of maximum compressive strain, which is simplified to be the moment when the subsequent layer above the layer under consideration has just been completed. The time at which the entire wall has been built and has completely cooled down is selected as t_2.

2.6. Development of Own Approach

In order to provide a further basis for investigating how the inherent strain can be extracted from the thermomechanical simulation, all strains occurring on a single element in the centre of the first layer of the wall are measured over the entire time of the build job, irrespective of arbitrarily selected time points. The output of elastic strain, plastic strain, and thermal strain is thus analyzed.

3. Results and Discussion

3.1. Inverse Calibration of the Inherent Strain

The result of the thermomechanical calculation is shown in Figure 2A, which serves as a reference for further comparison. From a purely qualitative point of view, it is noticeable that the distortion is relatively symmetrical. The distortion is shown in the graphical representation at both ends of the wall as an approximate semicircle. The maximum and minimum distortion values of +0.23 mm and −0.23 mm, respectively, can be found relatively centred at each end of the wall, but with a slight tendency towards the lower half of the wall.

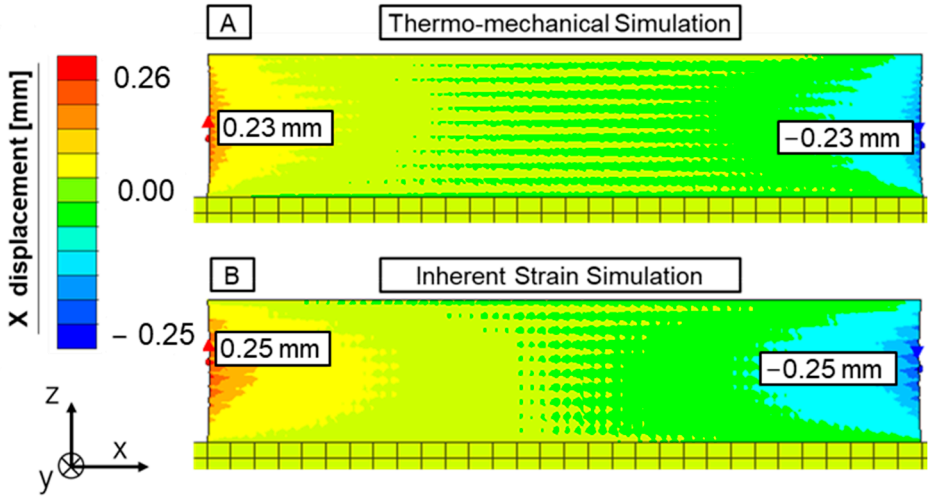

Figure 2. Comparison of the results of the thermomechanical simulation (**A**) and the inherent strain simulation (**B**) using an inverse defined constant inherent strain $\varepsilon^{IS} = -0.024$.

The result of the inherent strain calculation using an inherent strain $\varepsilon^{IS} = -0.024$ is shown in Figure 2B. In a purely qualitative view of the results, the result of the thermomechanical calculation is very well reproduced. The distortion is expressed in the graphical representation as a semicircle at each end of the wall. The quantitative analysis results in maximum and minimum distortion values of 0.25 mm and −0.25 mm, respectively, which represents a deviation of approx. 8% compared to the thermomechanical calculation. This leads to the conclusion that the inherent strain calculation result has an accuracy of 92% of the comparative thermomechanical simulation.

This shows that the distortion of a thermomechanical calculation can be modelled with relatively good accuracy (92%) using an inherent strain calculation with a constant

inherent strain. At the same time, the calculation time was reduced from 8 h for the thermomechanical calculation to 3 h for the inherent strain calculation.

Similar results can be found in the literature. Liang and Duan [10,11,14], for example, were able to calculate the distortion values of a thermomechanical simulation using an inherent strain calculation with a constant inherent strain value in several works. However, in contrast to Liang and Duan, in this work, the built geometry itself was considered rather than the substrate plate. Chen et al. [16] were also successful with an inverse determination and were thus able to reproduce the distortion of a substrate plate with a constant inherent strain. Considering the uncertainties in the material parameters, process parameters, and boundary conditions, the result values for the inherent strain in this work being in the same order of magnitude as the values found in the literature can be regarded as a good agreement. This substantiates the methodology described in this work.

A comparison of all identified inherent strains is listed in Table 1.

Table 1. Comparison of inherent strain values from the literature.

Author	Longitudinal	Transverse	Height	Calculation Method	Geometry	Material
This Work	−2.40%	0.0%	0.0%	Inverse identified	30-layer wall	316 L
Liang [11]	−1.3%	−0.3%	1.2%	MIS	5-layer wall 10-layer square frame	Ti64
Duan [12]	−0.1%	−0.1%	0.2%	MIS	2-layer wall, cam	316 L
Duan [13]	−0.6%	0.2%	0.3%	MIS	8-layer wall	12CrNi2
Duan [14]	−1.0%	−2.9%	3.8%	MIS	8-layer wall 5-layer square frame	12CrNi2
Bellet [15]	−1.5%	0.1%	1.0%	Own approach	8-layer turbine mockup	316 L
Dong [22]	−0.5%	−1.0%	0.8%	Temperature-dependant MIS	3-layer wall	Ti64
Ye [17]	−0.4%	0.7%	4.7%	Inverse identified	20-layer wall	In718
Ye [17]	−1.3%	0.4%	2.7%	Inverse identified	20-layer wall	IN625
Chen [16]	−0.5%	−2.4%	3.1%	Inverse identified	2-track and 2-layer wall 4-track and 3-layer wall 4-track and 6-layer square frame	316 L

3.2. Testing of Common Approaches

The results of the calculation of the classic and modified inherent strain are shown in Figure 3. It should be mentioned again that the classic inherent strain is equal to the plastic strain at the time when the whole structure has cooled to room temperature (in this work marked as t_2), and the modified inherent strain consists of the plastic strain at the time when the subsequent layer is finished minus the difference in elastic strains between these two points in time.

The classic inherent strain (CIS) shows boundary effects at the beginning of the welded wall, and the calculated CIS is in the positive range with a relatively high value of 0.05. Within a few elements, however, it sinks to a relatively constant value of around −0.01 before rising sharply again towards the end of the wall. The positive value of the CIS at both ends of the wall does not correspond to the expected value. The general expectation of the behaviour of the material after welding or a DED build-up is for the material to shrink because of cooling. A shrinkage of the material would be described by a negative strain value. However, there are positive strains present which would indicate an expansive behaviour of the material which should not be present. Since positive values are only present at the edges of the wall, these should be considered edge effects. The negative strain in the majority of all measurement points do correspond to the expectation that a

component will shrink due to cooling and therefore experience distortion due to irregular restraints to shrinkage.

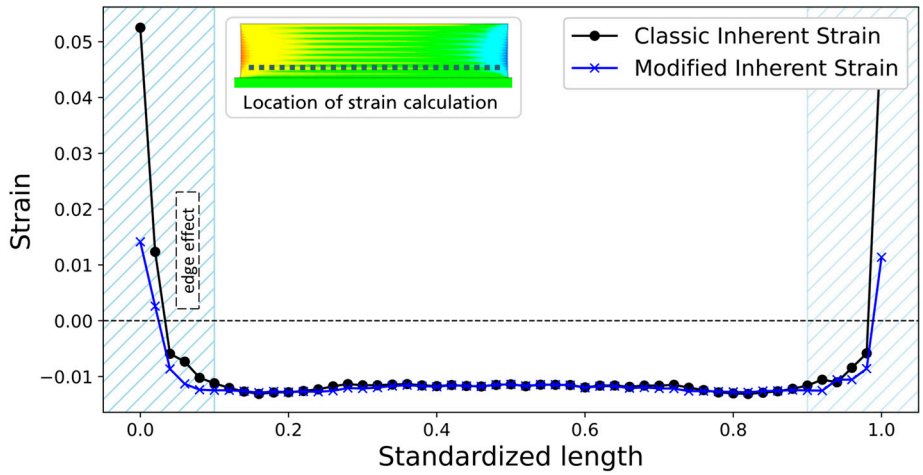

Figure 3. Calculation of the classic inherent strain and the modified inherent strain, calculated for every fourth numeric element of the first layer of the wall (as indicated by the dotted line: location of strain calculation) and plotted over the standardized length of the first layer, extracted from the thermomechanical simulation.

The modified inherent strain also exhibits edge effects. Positive values of 0.01 can be observed at the beginning of the wall, after which the value drops to approx. −0.01. Here, too, positive values can be found at the edges of the wall, whereas negative values tend to be found towards the centre of the wall. The previously mentioned edge effect also appears to be observable here. Figure 4 shows the individual plastic and elastic strains at the two selected points in time, which are used for the calculation of the CIS and MIS in Figure 3.

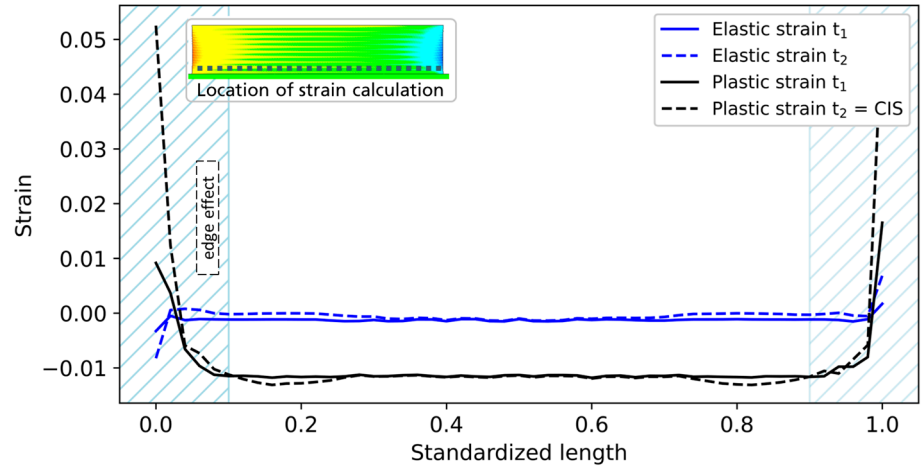

Figure 4. Visualization of the elastic and plastic strain at the two points in time t_1 and t_2 over the length of the entire wall. t_1 is the point in time when the subsequent layer above the layer under consideration has just been completed, and t_2 is the time at which the entire wall has been built and has completely cooled down in accordance with Liang [10]. The dotted line in the graphical representation of the wall indicates the location where both strains were calculated. Both strains were calculated for every fourth element in the first layer of the build-up. The plastic strain at t_2 corresponds with CIS in Figure 3.

When examining the two graphs for the elastic strain, it is noticeable that there is no significant difference between the values of the elastic strain for both points in time. For

both graphs, the elastic strain fluctuates around the zero value, with the exception of the values at both ends of the wall, which peak at absolute maximum values of 0.002. These can be considered edge effects, analogous to the previous inspection of the peaks of the CIS and MIS in Figure 3. This means that the elastic strain, compared to the values of the plastic strain, has a negligible influence on the calculation of the MIS. Liang's [10] assumption that the difference in the elastic strain between the two points in time is a correction factor that can map the changing geometric boundary conditions does not appear to apply in the case of the wall and the process analyzed here.

The plastic strain takes on a higher value in terms of magnitude over its course at both points in time and is therefore largely responsible for the course of the MIS in Figure 3. Simultaneously, similarly to the elastic strain, there is no significant difference between the plastic strains for the two points in time. Apart from the high values at both ends of the walls, which are likely distorted due to edge effects, the value of the plastic strain fluctuates around −0.01.

The next question is whether the CIS or the MIS can be used to determine the value of the inversely identified inherent strain ε^{IS} in this work. For this purpose, the average value of the CIS and MIS are calculated to obtain a comparative value that is analogous to Liang's work [10]. In order to exclude the influence of boundary effects, an average value is also calculated without the outer five FE nodes. The result is listed in Table 2.

Table 2. Averaged values for the calculated classic (CIS) and modified inherent strain (MIS).

CIS	CIS Without Boundary Effects	MIS	MIS Without Boundary Effects
−0.009	−0.011	−0.011	−0.012

The values for the CIS (−0.9% and −1.1%) do not correspond with the value for the inversely determined inherent strain ε^{IS} = −2.4% in both cases, with and without the outer FE nodes. This means that the values of the CIS can not be used to replicate the desired distortion of a thermomechanical simulation of this DED process. This goes in line with previous investigations. Liang [10] was also not able to replicate the distortion of a thermomechanical simulation using the CIS theory—which was also only developed for use within welding technology, not additive manufacturing. This then actually led to the further development of the inherent strain theory into the MIS theory by Liang [10]. The further application of the CIS on DED processes could not be found by the authors since most work is either based on the MIS theory or uses an inverse determination of the inherent strain.

The method of MIS was successful in previous investigations [10,11,23]. Here, the MIS theory could provide a value for the inherent strain which then could replicate the distortion of a thermomechanical simulation using an inherent strain simulation. In contrast to these sources, the MIS approach does not work for the process in the present work. The MISs that have been calculated for the present process have values of −1.1% and −1.2. which do not correspond to the inversely determined ε^{IS} = −2.4%. There are several possible explanations why the theory is not applicable in this case.

The initial theory of the modified inherent strain relies on the assumption that the initial time step t_1 is selected to be the time point of maximum compressive strain, which is simplified to be the moment when the subsequent layer above the layer under consideration has just been completed. Naturally, the moment the heat source passes the element under consideration, the highest compressive strains are present, which should be responsible for distortion. If the heat source moves a long distance or for a long time, e.g., in a process involving a very long wall and/or very slow welding speeds, the moment the subsequent layer is finished might not correspond to the moment of the highest compressive strain and therefore might not depict the physical basis for distortion in a reasonable manner. It is possible that the MIS theory only applies to certain combinations of component geometry and process parameters, e.g., short walls or processes involving high welding speeds.

Another possible explanation is the type of inherent strain application. In this work, an element-by-element application of the inherent strain was used, whereas in all of the existing literature, a layer-by-layer application of the inherent strain is performed. During the application of the inherent strain and the activation of singular elements, there are settlement processes where the strain of every single element is calculated against every newly activated element. When comparing this process to the activation of a whole layer, it makes sense that the layer-by-layer variant might require lower strain values to produce the desired distortion.

Independent of the reasons of the MIS theory not being applicable in this investigation, a new approach to physically calculate the desired inherent strain needs to be evaluated. Using the current theories, it is not possible to achieve values for the inherent strain which correspond to the inversely determined inherent strain, which was able to recreate the desired distortion from a thermomechanical simulation. Since the current theories provide inherent strain values around -0.1%, which is only approx. 40% of the value of the inversely determined inherent strain of -2.4%, which is needed to achieve the desired distortions, it is evident that the current theories are not applicable to the process studied.

3.3. Thermal Strain as a Basis for a New Inherent Strain Method

In Figure 5, the elastic, plastic, and thermal strains from the thermomechanical model are plotted over time. In addition, the inversely determined inherent strain $\varepsilon^{IS} = -0.024$ is plotted in green. All three strains behave cyclically where there are regular increases and decreases. The cyclical jumps occur simultaneously for all three strains and correspond to the influence of the heating and cooling of additional individual welded layers. The first rise or fall therefore corresponds to the welding of the first layer; all further cyclical changes represent the influence of the subsequently welded layers. As the additionally welded layers are further and further away from the first layer, the influence in the form of spikes is reduced and the values converge towards a fixed value.

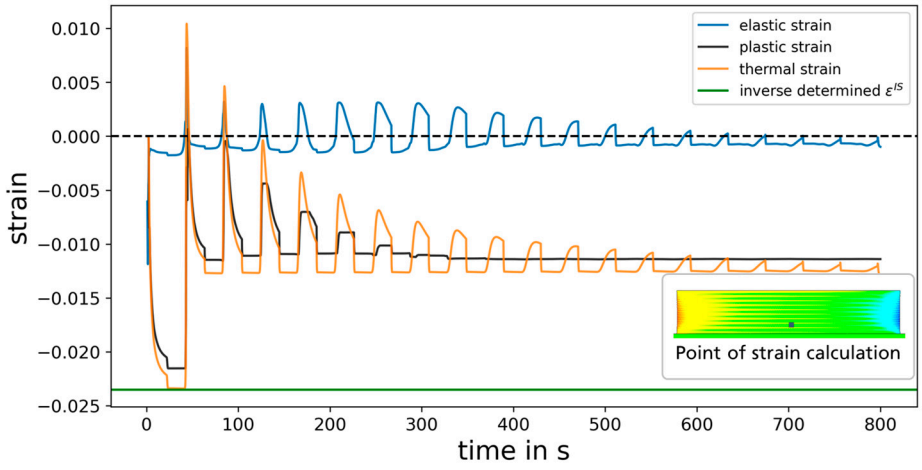

Figure 5. Elastic, plastic, and thermal strain, extracted form an element in the centre of the first layer, plotted over the time of the whole build-up.

The thermal strain is, apart from a few peaks in the positive range, largely in the negative range and is therefore compressive in nature. This corresponds to the expectation that numeric elements that are welded shrink due to cooling and therefore compress. The individual local minima of thermal expansion are cyclically followed by local maxima. These are caused by a combination of the cooling of the numeric element and the effect of the tensile stresses of the applied compressive strain of the subsequently applied numeric elements. This also explains the short jumps into the positive range. The plastic and elastic strain behave analogously to the thermal strain, whereas the values are lower.

As a singular strain value, thermal strain is the largest value occurring in the simulation and amounts quantitatively to the sum of plastic and elastic strain. This also corresponds to the expectation, as the thermal strain from welding is first converted into elastic strain until the yield point is reached and then converted into plastic strain. In this model, thermal strain is the only strain considered; other effects, i.e., from phase transformation, are neglected as the 316 L steel remains fully austenitic.

Finally, the minimum of the thermal strain comes very close to the inversely determined inherent strain $\varepsilon^{IS} = -0.24$ and seems to offer a possibility to provide a constant inherent strain ε^{IS} without inverse determination and time-consuming trial and error, which can be extracted directly from a thermomechanical simulation. The thermal strain provides a characteristic value for the process, which appears to represent the distortion in a meaningful way in an inherent strain calculation. This can be assumed to be characteristic because the thermal strain is dependent on both the heat introduced, i.e., the process variables, and the heat dissipated, i.e., the geometric boundary conditions, material properties, etc.

Figure 6 shows the behaviour of the minimum thermal strain over the entire length of the first layer. The value stays constant around the value of -0.0245, with the exception of outliers in the area of the ends of the wall, which can be considered boundary effects. It can therefore be concluded that the minimum thermal expansion does not change significantly with the exception of the edge effects. The mean value determined here comes very close to the inversely determined inherent strain $\varepsilon^{IS} = -0.024$. Due to no visible deviation or fluctuation, the conclusion can be drawn that the minimal thermal strain is approximately the same for every element over the entire first layer.

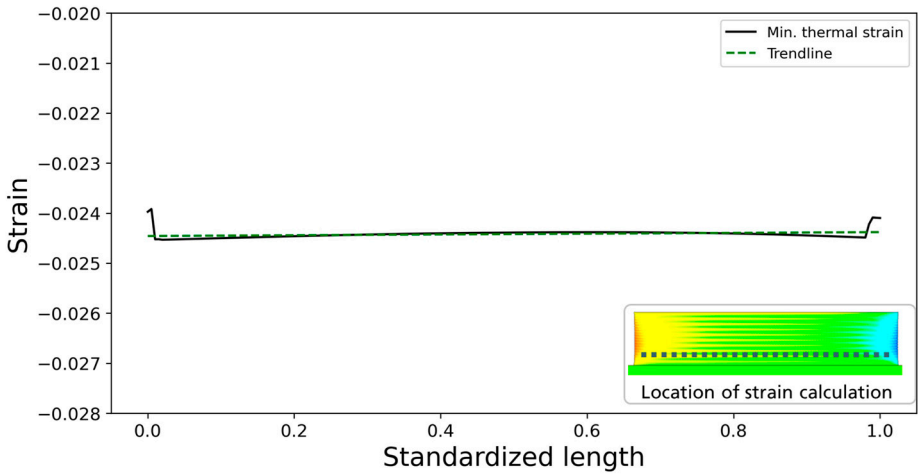

Figure 6. Assessment of the progression of the minimal values for thermal strain for every single FE in the first layer.

3.4. Choice of Thermal Expansion as the Basis of the Inherent Strain

In this study, the value of the minimum of the thermal strain comes very close to the inversely determined inherent strain. In addition to the correspondence of the quantitative amount, it must also be considered whether the thermal strain is useful in comparison with the previous approaches of considering the plastic and elastic strain in the literature [10,13,22].

Generally, thermally induced strain and then restricted shrinkage is the cause of distortion. Thermal strain, which results from the characteristic thermal expansion coefficient as well as the temperature to which the material is heated and the temperature to which it is cooled, is therefore a measure of the cause of distortion. Since the temperatures reached in the process depend on the heat input and the heat dissipation, the thermal strain should be characteristic for the respective application. During the DED process, the initial thermal strain is split into plastic and elastic strains during the cooling process, according to the

material modelling. Naturally, the thermal expansion decreases to zero at the end of the process, but the moment of the highest temperature is largely responsible for the resulting distortion. Thus, in contrast to the considerations of Yuan and Liang [9,10], the authors of this work do not consider thermal expansion to be negligible. Rather, since the thermal strain is the cause of the plastic and elastic strain, it appears to provide a reliable physical basis for the inherent strain in the example analyzed. It seems reasonable to use the thermal strain as the basis for calculating the inherent strain rather than the elastic and plastic strain values at arbitrarily chosen time points, which result from the thermal strain and therefore represent a physical variable that comes one step later in the causal chain of effects, respectively, and are calculated from the thermal strain.

4. Conclusions

- A model consisting of a single-track wall with 20 layers was used to compare the calculated distortion of a thermomechanical simulation and an inherent strain simulation using an element-by-element application of the inherent strain.
- A constant ε^{IS}, inversely determined in an iterative manner from inherent strain calculations, can be used to accurately reproduce the distortion calculated by a thermomechanical solution using the single-track wall.
- The classic inherent strain and the modified inherent strain do not correspond to the inversely determined inherent strain. Assumptions made in the literature regarding the timing of data extraction do not appear to be valid in the case of the analyzed process parameters, geometry, and inherent strain application.
- The minimal value of the thermal strain in the first layer corresponds to the inversely determined inherent strain.
- The thermal strain gives a physical basis for the inherent strain and can be used as a basis to accurately calculate the distortion of a 20-layer-high, single-track wall.
- The determination of the inherent strains has only been made using the first layer of a single-track wall. Before applications to complex industrial parts can be made further, a study of the dependence of the location of the investigated elements and the application on massive components needs to be made.

Author Contributions: Conceptualization, G.S. and M.B.; methodology, G.S., P.B. and B.A.M.E.; software, G.S., P.B. and B.A.M.E.; validation, G.S. and P.B.; formal analysis, G.S. and P.B.; investigation, G.S., P.B. and M.B.; resources, M.R. and M.B.; data curation, G.S. and M.B.; writing—original draft preparation, G.S.; writing—review and editing, G.S.; visualization, P.B.; supervision, M.R. and M.B.; project administration, G.S. and M.B.; funding acquisition, M.R. and M.B. All authors have read and agreed to the published version of the manuscript.

Funding: The research project P 1468 "Mechanical replacement models for the rapid simulation of large DED structures" from the Research Association for Steel Application (FOSTA), Düsseldorf, was supported by the Federal Ministry of Economic Affairs and Climate Action through the German Federation of Industrial Research Associations (AiF) as part of the programme for promoting industrial cooperative research (IGF) on the basis of a decision by the German Bundestag. The project was carried out at Fraunhofer IPK, Berlin.

Data Availability Statement: The datasets presented in this article are not readily available because the data are part of an ongoing study.

Conflicts of Interest: Beatrix Elsner was employed by the Hexagon Manufacturing Intelligence GmbH. The remaining authors declare that the research was conducted in the absence of any commercial or financial relationships that could be construed as a potential conflict of interest.

References

1. Frazier, W.E. Metal Additive Manufacturing: A Review. *J. Mater. Eng. Perform.* **2014**, *23*, 1917–1928. [CrossRef]
2. Svetlizky, D.; Das, M.; Zheng, B.; Vyatskikh, A.L.; Bose, S.; Bandyopadhyay, A.; Schoenung, J.M.; Lavernia, E.J.; Eliaz, N. Directed energy deposition (DED) additive manufacturing: Physical characteristics, defects, challenges and applications. *Mater. Today* **2021**, *49*, 271–295. [CrossRef]

3. Papadakis, L.; Hauser, C. Experimental and computational appraisal of the shape accuracy of a thin-walled virole aero-engine casing manufactured by means of laser metal deposition. *Prod. Eng.* **2017**, *11*, 389–399. [CrossRef]
4. Amar, E.; Popov, V.; Sharma, V.M.; Andreev Batat, S.; Halperin, D.; Eliaz, N. Response Surface Methodology (RSM) Approach for Optimizing the Processing Parameters of 316L SS in Directed Energy Deposition. *Materials* **2023**, *16*, 7253. [CrossRef] [PubMed]
5. Biegler, M.; Elsner, B.A.M.; Graf, B.; Rethmeier, M. Geometric distortion-compensation via transient numerical simulation for directed energy deposition additive manufacturing. *Sci. Technol. Weld. Join.* **2020**, *25*, 468–475. [CrossRef]
6. Biegler, M.; Graf, B.; Rethmeier, M. Assessing the predictive capability of numerical additive manufacturing simulations via in-situ distortion measurements on a LMD component during build-up. *Procedia CIRP* **2018**, *74*, 158–162. [CrossRef]
7. Marimuthu, S.; Clark, D.; Allen, J.; Kamara, A.; Mativenga, P.; Li, L.; Scudamore, R. Finite element modelling of substrate thermal distortion in direct laser additive manufacture of an aero-engine component. *Proc. Inst. Mech. Eng. Part C J. Mech. Eng. Sci.* **2013**, *227*, 1987–1999. [CrossRef]
8. Biegler, M.; Khazan, P.; Gazen, M.; Rethmeier, M. Improvement of numerical simulation model setup and calculation time in additive manufacturing-laser-metal-deposition compontents with an advanced modelling strategy. In *Mathematical Modelling of Weld Phenomena 12*; Verlag der Technischen Universität Graz: Graz, Austria, 2019; Volume 2019, pp. 979–1003. [CrossRef]
9. Yuan, M.G.; Ueda, Y. Prediction of Residual Stresses in Welded T- and I-Joints Using Inherent Strains. *J. Eng. Mater. Technol.* **1996**, *118*, 229–234. [CrossRef]
10. Liang, X.; Chen, K.P.; Chen, Q.; Cheng, L.; Yang, Q.; To, A.C. A Modified Inherent Strain Method for Fast Prediction of Residual Deformation in Additive Manufacturing of Metal Parts. In Proceedings of the 2017 International Solid Freeform Fabrication Symposium, Austin, TX, USA, 7–9 August 2017. [CrossRef]
11. Liang, X.; Cheng, L.; Chen, K.P.; Chen, Q.; Yang, Q.; To, A.C. A modified method for estimating inherent strains from detailed process simulation for fast residual distortion prediction of single-walled structures fabricated by directed energy deposition. *Addit. Manuf.* **2018**, *23*, 471–486. [CrossRef]
12. Duan, C.H.; Cao, X.K.; Zhao, M.H.; Luo, X.P. Research on Deformation Prediction Method of Laser Melting Deposited Large-Sized Parts Based on Inherent Strain Method. *Key Eng. Mater.* **2021**, *871*, 65–72. [CrossRef]
13. Duan, C.; Cao, X.; Luo, X. Efficient Distortion Prediction of Laser Melting Deposited Industrial-scale Parts Using Modified Inherent Strain Method. *IOP Conf. Series Earth Environ. Sci.* **2021**, *714*, 032032. [CrossRef]
14. Duan, C.; Cao, X.; Luo, X. Efficient distortion predictions of high-performance steel alloy parts fabricated by pragmatic deposition strategies in laser melting deposition. *J. Laser Appl.* **2022**, *34*, 012010. [CrossRef]
15. Bellet, M.; Keumo Tematio, J.W.; Zhang, Y. Critical Assessment of the Inherent Strain Method for Thermo-Mechanical Simulation of Additive Manufacturing and Proposed Alternative: The Inherent Strain Rate Method. 9 November 2022, Rochester, NY: 4272651. Available online: https://papers.ssrn.com/abstract=4272651 (accessed on 13 January 2023).
16. Chen, Y.; Xu, Y.; Hou, L.; Shao, W.; Jing, X.; Li, Y.; Chen, S. Fast distortion prediction in directed energy deposition using inversely-identified inherent strains. *J. Eng. Des.* **2023**, *34*, 294–312. [CrossRef]
17. Ye, C.; Chen, Y.; Hou, L.; Xu, Y.; Li, Y.; Guo, J. Deformation prediction of functionally graded materials in laser directional energy deposition using forward-inverse calibration of the inherent strain in multi-scanning directions. *Appl. Opt.* **2023**, *62*, 2168. [CrossRef] [PubMed]
18. Hexagon. *Simufact Welding*; Hexagon Manufacturing Intelligence GmbH: Vienna, Austria, 2024.
19. Biegler, M.; Graf, B.; Rethmeier, M. In-situ distortions in LMD additive manufacturing walls can be measured with digital image correlation and predicted using numerical simulations. *Addit. Manuf.* **2018**, *20*, 101–110. [CrossRef]
20. *DIN ISO/TS 18166:2016*; Numerical Welding Simulation—Execution and Documentation (German Version). Deutsches Institut für Normung: Berlin, Germany, 2016.
21. Biegler, M.; Elsner, B.A.M.; Neubauer, I.; Lemke, J.; Rethmeier, M. Result quality evaluation of Directed Energy Deposition Additive Manufacturing simulations with progressive simplification of transient heat-source motion. *Procedia CIRP* **2022**, *111*, 277–281. [CrossRef]
22. Dong, W.; Jimenez, X.A.; To, A.C. Temperature-dependent modified inherent strain method for predicting residual stress and distortion of Ti6Al4V walls manufactured by wire-arc directed energy deposition. *Addit. Manuf.* **2023**, *62*, 103386. [CrossRef]
23. Liang, X.; Chen, Q.; Cheng, L.; Hayduke, D.; To, A.C. Modified inherent strain method for efficient prediction of residual deformation in direct metal laser sintered components. *Comput. Mech.* **2019**, *64*, 1719–1733. [CrossRef]